frontiers | Frontiers in Built Environment

TYPE Original Research
PUBLISHED 04 April 2023
DOI 10.3389/fbuil.2023.1156261

OPEN ACCESS

EDITED BY
Abdelhalim Azam,
Mansoura University, Egypt

REVIEWED BY
Ahmed Ehab Mostafa,
Badr University in Cairo, Egypt
Hadee Mohammed Najm,
Aligarh Muslim University, India
Manish Kumar,
SRM Institute of Science and Technology, India
Mohamed Mortagi,
Mansoura University, Egypt

*CORRESPONDENCE
Ahmed M. Yosri,
ahmedyosri204@gmail.com

SPECIALTY SECTION
This article was submitted to Construction Materials, a section of the journal Frontiers in Built Environment

RECEIVED 01 February 2023
ACCEPTED 24 February 2023
PUBLISHED 04 April 2023

CITATION
Alzara M, Yosri AM, Yousef SEAS and Deifalla AF (2023), Response of high-strength concrete beams with corrugated discrete steel fibers to small shear span-depth ratios.
Front. Built Environ. 9:1156261.
doi: 10.3389/fbuil.2023.1156261

Response of high-strength concrete beams with corrugated discrete steel fibers to small shear span-depth ratios

Majed Alzara[1], Ahmed M. Yosri[1]*, Saif Eldeen A. S. Yousef[2] and Ahmed Farouk Deifalla[3]

[1]Department of Civil Engineering, College of Engineering, Jouf University, Sakakah, Saudi Arabia, [2]Department of Civil Engineering, Faculty of Engineering, Al-Baha University, Al Bahah, Saudi Arabia, [3]Structural Engineering and Construction Management Department, Future University in Egypt, New Cairo, Egypt

The behavior of high-strength, fiber-reinforced concrete (HSFRC) beams under concentrated loads was affected by many different aspects, such as the type of fibers used and the volume percent of the fibers; nevertheless, the behavior was primarily affected by modifying the shear span-to-depth ratio (a/d). In this experimental investigation, the influence of a/d ratios (ranging from 1.5 to 2.2) is investigated on the response of twelve high-strength fiber-reinforced concrete (HSFRC) beams containing varying amounts of discontinuous steel fiber (vf) in the concrete mixture. The purpose of this study was to analyze the manner of failures of the tested beams and to identify a limiting a/d for effective beam depth. Shear failure was observed in high-strength concrete (HSRC) beams with a vf of 0% at a/d ratios as high as 2.2, according to the findings of the study. Altering either the a/d ratios or the vf had an effect on the way in which the HSFRC beams responded to the stimulus. Some of the HSFRC beams that were put through the shear–flexure test failed. In addition, the findings demonstrated that, as the a/d ratio increased up to 2.2, the beams with a vf of 0.5% and 0.75% broke in pure flexure with multi-cracking. This indicates that the a/d ratio has a substantial impact on the various failure behaviors of HSFRC beams.

KEYWORDS

high-strength, fiber-reinforced concrete, failure mode, shear span-to-depth ratio, fiber content

1 Introduction

High-strength concrete (HSC) has outstanding mechanical properties, such as a high resistance to compression stresses, a high modulus of elasticity (stiffness), a low permeability for harmful substances, and a high resistance to corrosion. These distinctive properties enable its use in diverse construction project applications, and it can be used in many prestressed concrete structures such as concrete bridges (Biolzi et al., 1997; Song and Hwang, 2004; Ozbakkaloglu, 2013; Lim and Ozbakkaloglu, 2014; Kou and Poon, 2015; Vincent and Ozbakkaloglu, 2015). High-strength con-crete is a brittle material, where there is an inverse relationship between concrete strength and ductility; therefore, there are many studies that deal with this issue. Some studies have added materials to the concrete mixture to improve and develop it. Some studies have shown that adding small discrete steel fibers can enhance the shear strength and toughness for high-strength concrete and improve its ductile,

also promoting its flexural failure (Toutanji et al., 2004; Jang et al., 2015; Yoo et al., 2017; Zhao et al., 2018; Choi et al., 2019; Lantsoght, 2019; Shahnewaz and Alam, 2020). Furthermore, distributing the discrete steel fibers lead to produce a bridging action across small-cracks in the mixture and improve the resistance for propagation of the cracks and crack opening.

The influence of adding fibers to a concrete mix depends on many factors, such as the fiber type, the fiber orientation in the mix, and the fiber geometry; the main factors are the fiber volume fraction (vf) and inclusion, and the properties of the fiber matrix (Savastano et al., 2006; Sudin and Swamy, 2006; Kuder and Shah, 2010; Cao and Khan, 2021). Fibers that can be used in a concrete mixture have many different types, and an effective fiber type is metallic fibers, such as carbon fibers or stainless-steel fibers, which have two shapes: hook-end fibers and corrugated fibers (Brandt, 1985; Kim and Park, 1994; Geng and Leung, 1996; Yurtseven, 2004; Ahmed et al., 2007; Perceka et al., 2019; Khan and Ali, 2020; Khan et al., 2021; Khan et al., 2022). The pullout behavior of steel fibers from concrete and the bond strength between steel fibers and concrete comprise complex problems; therefore, the shape of the fibers used is a very important factor to be considered when studying the behavior of high-strength fiber-reinforced concrete (HSFRC) beams subjected to two-point concentrated and monotonic loads.

Additionally, the shear span-to-depth ratio (a/d) has a major effect on the ultimate resistance of high-strength fiber reinforced concrete beams, as shown in previous studies. Some of these studies showed that for a/d smaller than 2.2 the ultimate strength of high-strength fiber reinforced concrete beams, is controlled by the capacity of the arch action because the arch action lead to transfers the load directly from the loading point to the pin support through a strut (a compressive strut) while for a/d greater than 2.2 the ultimate resistance mainly controlled by the flexural capacity of un-cracked concrete (Swamy and Bahia, 1985; Mansur et al., 1986; Dinh, 2009; Lin, 2013; Bae et al., 2021; Yun et al., 2022). Furthermore, a beam's shear strength becomes lower as the shear span-to-depth ratio increases (Dinh, 2009; Yun et al., 2022; ASTM C188-14, 2009).

As mentioned before, previous studies have dealt with the influence of changing the a/d ratio on the behavior of HSFRC beams, but the common fiber shape in these studies is a hook-end steel fiber, not a corrugated steel fiber, such as in studies by Swamy and Bahia (Bae et al., 2021) and Yun et al. (ASTM C188-14, 2009).

According to Swamy and Bahia (Bae et al., 2021), a fiber volume fraction of 0.5% leads to a change in the mode of failure of SFRC beams from a diagonal tension failure to a shear-compression failure, whereas a higher fiber volume fraction of more than 0.8% may cause the beams to fail in flexure mode. However, Yun et al. (ASTM C188-14, 2009) stated that the tensile strength of hook-end steel fibers significantly effects the shear strength of HSFRC beams, regardless of the shear span-to-depth ratio.

This research is important because it aims to determine the behavior of HSFRC beams reinforced with corrugated discrete steel fibers subjected to low shear span-to-depth ratios. We also wanted to look into the failure modes of HSFRC beams with different fiber contents in the concrete mix when subjected to these ratios. Twelve HSRFC beams of the same rectangular section were tested with a/d ratios of 1.5, 1.7, and 2.2 and vf values from 0 to 0.75 percent to see which combination produced the best results.

2 Materials and methods

2.1 Materials

2.1.1 Cement

Ordinary Portland cement was used, with a specific gravity of 3.15. The cement used was tested according to ASTM-C118 (ASTM C786/C786M-17, 2017) and its fineness modulus was tested according to ASTM C-184-94 (ASTM C 33-86, 1986). The properties of the cement used are shown in Table 1.

2.1.2 Aggregates

The coarse aggregate and the fine aggregate were sourced from local crushed stones and local natural sand. ASTM C-33 (ASTM C-127, 2001) and ASTM C-127 (ASTM C-128, 2001) were used for testing the coarse aggregate, while ASTM C-33 (ASTM C-127, 2001) and ASTM C-128 (ASTM A370, 2012) were used for testing the fine aggregate. The various properties of both of the coarse and the fine aggregates are listed in Table 2.

2.1.3 Steel fibers

In this study, one type of discrete steel fiber with a corrugated shape was used in the mix. The steel fibers were tested in accordance with ASTM A 370 (ASTM C469/C469M-10, 2010) to determine fiber tensile strength. The properties of the corrugated fibers are shown in Table 3, while the shape of the fibers is shown in Figure 1.

2.1.4 Main reinforcement

The longitudinal reinforcement used in this study was from high-tensile steel with a grade of 36/52. The 16 mm bars were used as longitudinal reinforcement, while the 8 mm bars were used as transverse reinforcement.

2.1.5 Concrete mix proportions

The appropriated high-strength concrete was produced with ordinary Portland cement, fine aggregate, coarse aggregate, superplasticizer, and silica fume. The silica fume had 2.23 specific gravity and 200,000 cm^2/gm surface area. The concrete target compressive strength was designed to be no less than 50 MPa. The concrete mix proportions are shown in Table 4.

2.2 Testing procedure

2.2.1 Overview of tested beams

In this study, tests were carried out on twelve HSRC beams with constant dimensions for each beam, with a fixed span of 1,500 mm and a rectangular cross-section 250 mm in depth and 120 mm in width, as shown in Figure 2.

These HSRC beams were divided into three groups (A, B, and C) according to the shear span-to-depth ratios of 1.5, 1.7, and 2.2, respectively. Each group contained four beams (S0, S1, S2, and S3); these numbers refer to the volume fraction of the used corrugated fiber

TABLE 1 Properties of the cement used.

Final setting time (min)	Initial setting time (min)	Fineness modulus	Specific gravity
250	80	340 m^2/kg	3.15

TABLE 2 Properties of the aggregates used.

Fineness modulus	Max aggregate size	Absorbtion capacity (%)	Bulk density	Specific gravity	Property
-----	37.5 mm	0.40	1,650.8 kg/m^3	2.65	Coarse Aggregate
2.6	------	1.20	------	2.15	Fine Aggregate

TABLE 3 Properties of corrugated fibers.

Ultimate tensile strength (MPa)	Ultimate tensile strain	Diameter (mm)	Length (mm)	Density (kN/m^3)
1,100	2.2	0.75	60	78.5

FIGURE 1
The corrugated fiber used.

TABLE 4 Concrete mix proportions.

Material	Weight
Cement	550 kg/m^3
Fine Aggregate	650 kg/m^3
Coarse Aggregate	1,050 kg/m^3
Silica fume (% of cement)	10%
Super plasticizer (L/100 kg of cement)	1.8
Water/Cement	0.3

by weight in the order of 0%, 0.25%, 0.5%, and 0.75%, respectively. The full details of the tested specimens are given in Table 5 and the volume fraction was calculated by the following equation:

$$v_f = v_{sf} / v_c$$

where v_{sf} is the volume fraction of corrugated steel fiber, and v_c is the specimen's volume.

2.2.2 Reinforcement details of specimens

The main longitudinal reinforcement in all test specimens consisted of 2 bars of 16 mm-diameter deformed steel, while the compression reinforcement consisted of 2 bars of 12 mm-diameter deformed steel. The shear reinforcement was mild steel stirrups. Figure 3 shows the details of the reinforcement of the tested beams.

Four-point loading tests were carried out on the beams in order to be able to estimate their shear and flexure strengths. A digital load cell with a capacity of 550 kN was used to measure the loads. The vertical displacement of the beams was recorded using three electric dial gauges, as shown in Figure 4.

3 Results

3.1 Compressive strength

The tests were conducted on both the HSRC and the HSFRC beams. The compressive strength tests were performed on cylinders 150 mm in diameter and 300 mm in height, according to ASTM C469 [40]. Table 6 shows the concrete compressive strengths with different v_f. The results showed that the corrugated steel fibers had a visible effect on the concrete strength and concrete ductility.

The compressive strength of high-strength concrete increased from 51 MPa to 55.8 MPa due to the addition of corrugated steel fibers. The highest value for strength was

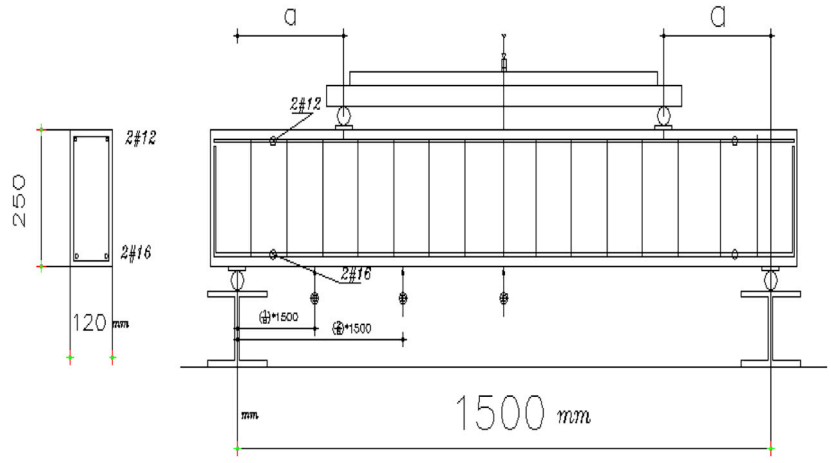

FIGURE 2
Beam specimen geometry.

TABLE 5 Overview of tested beams.

Top RFT	Main RFT	Stirrups	Volume of fraction (v_f) (%)	Specimens	Group
2D12 mm	2D16	7Φ8/m	0	A-0 (HSRC)*	A a/d = 1.5
			0.25	A-1(HSFRC) **	
			0.5	A-2 (HSFRC)	
			0.75	A-3 (HSFRC)	
			0	B-0 (HSRC)	B a/d = 1.7
			0.25	B-1(HSFRC)	
			0.5	B-2 (HSFRC)	
			0.75	B-3 (HSFRC)	
			0	C-0 (HSRC)	C a/d = 2.2
			0.25	C-1(HSFRC)	
			0.5	C-2 (HSFRC)	
			0.75	C-3 (HSFRC)	

* HSRC—high-strength reinforced concrete beams; ** HSFRC—high-strength, fiber-reinforced concrete beams.

noted for a v_f of 0.75%, which was 35.09% higher compared with the mix with a v_f of 0%.

3.2 Load–displacement response

Table 7; Figure 5 show the load versus the deflection of Group A beams with a/d ratios of 1.5. Increasing the ratio of the corrugated steel fiber enhanced the stiffness of the beams and enhanced the load-resisting capacity. The initial lateral stiffness of the A-0 HSRC specimen was 65.56 kN/mm, which increased to 70.45, 97.06, and 110.0 kN/mm for A-1, A-2, and A-3, respectively. The stiffness of the beams was improved by about 67.7% for the HSFRC beam with a v_f of 0.75% as compared with the HSRC beam without fibers. Table 8; Figure 6 show the load–deflection of the tested beams with a/d ratios of 1.7. Except for B-0, all the HSFRC beams exhibited similar load–deflection responses with significant post-yield deformation until their failure. Both B-2 and B-3 (HSFRC) beams with v_f values of 0.50% and 0.75%, respectively, presented the maximum load-resisting capacity as compared with the other beams. As shown in Table 9; Figure 7, the load vs. deflection response of Group C, with a/d ratios of 2.2, was nearly similar to that of Group B. The initial stiffness of the C-0 beam was 47.06 kN/mm, which increased to 55.45 kN/mm for the C-3 beam. This indicated that there was an 18% increase in the stiffness because of the addition of corrugated steel fibers to the mixture. As observed from the results, the increase in the a/d ratio led to a decrease in the peak load resistance for the beams and

FIGURE 3
Reinforcement details.

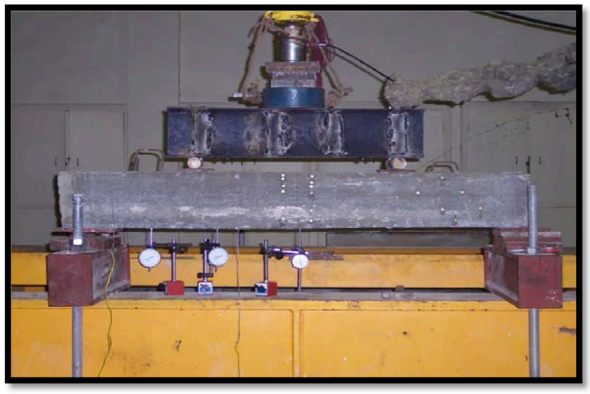

FIGURE 4
Test setup.

TABLE 6 Compressive strength.

Compressive strength (MPa)	Volume fraction (v_f) (%)
51	0
53	0.25
55.8	0.50
68.9	0.75

TABLE 7 Initial stiffness for the tested beams (a/d = 1.5).

Increment ratio	Stiffness (kN/mm)	Beam
0	65.56	A-0
7.40%	70.45	A-1
48.00%	97.06	A-2
67.70%	110.00	A-3

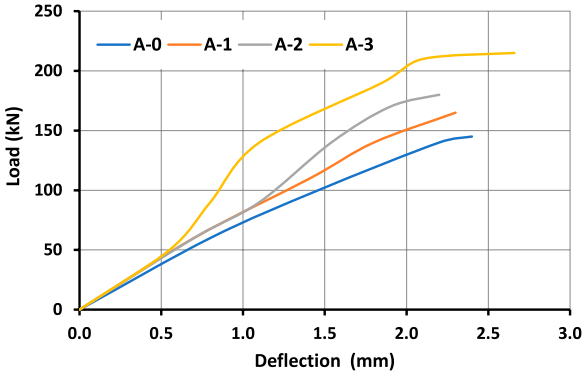

FIGURE 5
Load vs. deflection for the tested beams (a/d = 1.5).

TABLE 8 Initial stiffness for the tested beams (a/d = 1.7).

Increment ratio	Stiffness (kN/mm)	Beam
0	46.43	B-0
4%	48.21	B-1
7.70%	50.00	B-2
8.40%	50.32	B-3

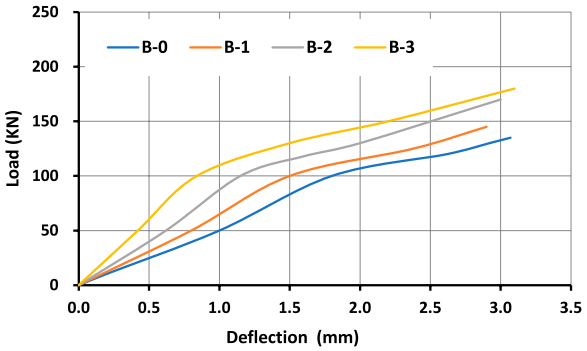

FIGURE 6
Load vs. deflection for the tested beams (a/d = 1.7).

TABLE 9 Initial stiffness for the tested beams (a/d = 2.2).

Increment ratio	Stiffness (kN/mm)	Beam
0	47.06	C-0
3%	48.26	C-1
10.00%	51.82	C-2
18%	55.45	C-3

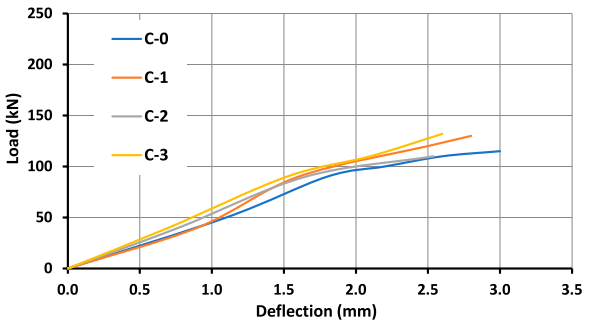

FIGURE 7
Load vs. deflection for the tested beams (a/d = 2.2).

TABLE 10 Summary of failure loads and mode of failure for all tested beams.

Mode of failure	Failure load (kN)	Beam
Shear–failure	145	A-0
Shear–failure	165	A-1
Shear–failure	180	A-2
Shear–failure	215	A-3
Shear–failure	135	B-0
Shear–failure	155	B-1
Shear–tension failure	170	B-2
Shear–tension failure	195	B-3
Shear–failure	115	C-0
Shear–compression Failure	130	C-1
Flexure Failure	148	C-2
Flexure Failure	160	C-3

increased the deformability. The orientation of the steel fibers also influenced the ultimate resistance and ductility of the HSFRC beams.

3.3 Load-resisting capacity

Table 10 shows the ultimate loads that were resisted by the tested beams. The values for the first-crack-correspondent loads for the HSRC specimens varied from 80 kN to 115 kN under all a/d ratios. The magnitude of the first-crack load for the HSFRC beams with a v_f of 0.25% decreased to 111 kN for a/d ratios of 2.2.

For the beams with an a/d ratio of 2.2, the magnitude of the first-crack load for the HSRC beams without fibers was 80 kN. This value increased to 122 kN for the HSFRC beams with a v_f of 0.75%, indicating an increase of about 52.5% due to the corrugated steel fibers.

As expected from previous studies, the ultimate loads for the HSFRC beams were higher than those for the HSRC beams for all a/d ratios. The A-0 beam exhibited an ultimate load of 145 kN, which increased to 215 kN for the A-3 beam, with an increment of 48.3%. Similarly, we observed a corresponding increment of about 44.4% for the HSFRC specimen with an a/d ratio of 1.7. Furthermore, at the a/d ratio of 2.2, the ultimate resistance of the HSFRC beams increased by 39.13% compared with the HSRC beams with a v_f of 0%.

As expected from previous studies, an increase in the a/d ratio caused a reduction in the magnitude of the ultimate load capacity of the beams, in addition to an increment in the ultimate deflection until their failure.

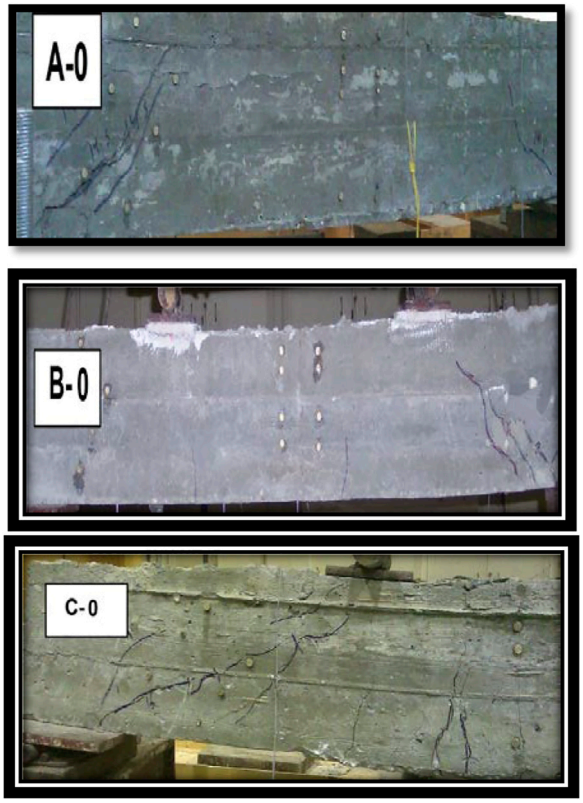

FIGURE 8
Propagation of cracks and modes of failure for HSRC specimens with varying a/d ratios.

3.4 Failure modes

The propagation of cracks and the modes of failure of HSRC beams with varying a/d ratios are shown in Figure 8. For the A-0 beam, there were diagonal cracks in the end segments at a load of 95 kN, in addition to minor flexural cracks in the mid-span regions. Shear cracks showed in the support regions at a magnitude of load of 118 kN. The width of this shear increased with increasing load levels. At failure, the diagonal tension (shear) failure happened as a result of the emanation of the diagonal cracks that roughly emanated from the supports, with an angle of 45°. As the a/d ratio increased to 1.7 and 2.2, the same shear cracks were noticed with different load values. There

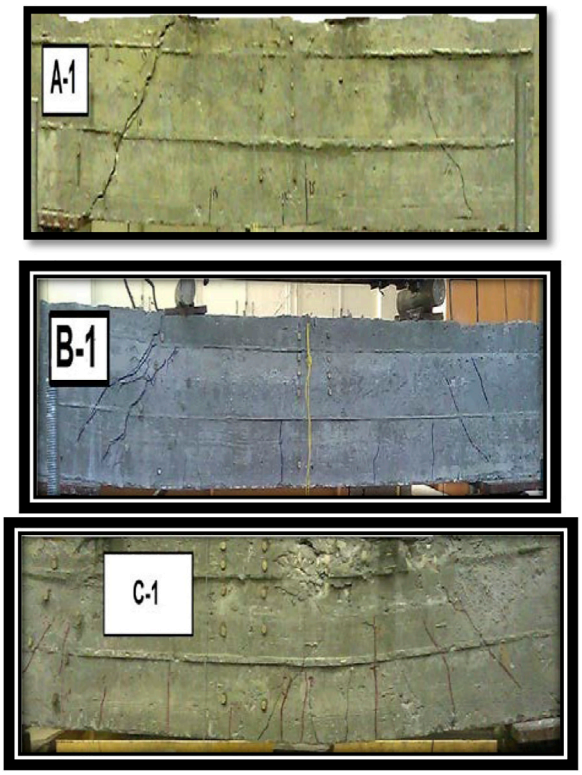

FIGURE 9
Propagation of cracks and modes of failure for HSFRC beams with a v_f of 0.25% and varying a/d ratios.

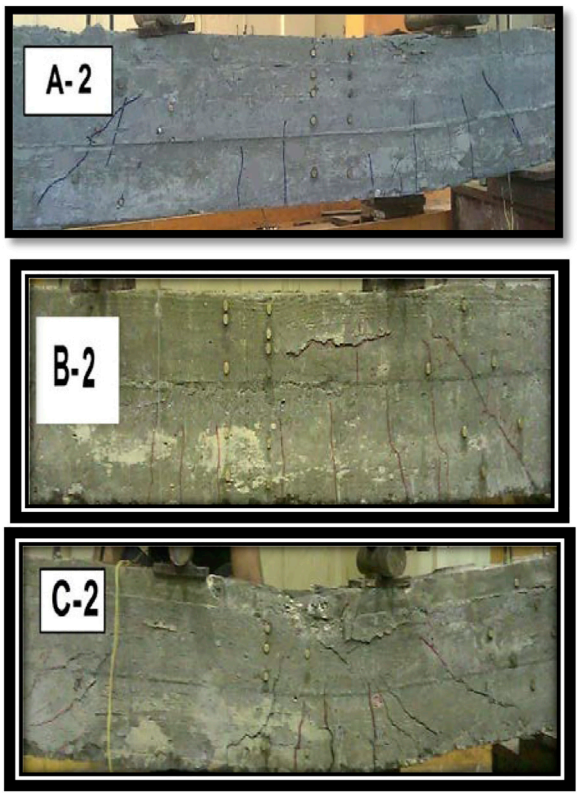

FIGURE 10
Propagation of cracks and modes of failure for HSFRC beams with a v_f of 0.5% and varying a/d ratios.

was no difference in either the mode of failure or the propagation of cracks in the HSRC beams with a/d ratios of 1.7 and 2.2, as shown in Figure 9. Additionally, from the results, the beam C-1 failed by shear–compression. The propagation of cracks and the failure mechanism for the HSFRC beams with a v_f of 0.75% are shown in Figure 10. As compared with the HSRC beams, the HSFRC beams showed a larger number of minor-cracks until failure. As the a/d ratio of the HSFRC increased to 2.2, a large number of major flexural cracks were noticed. At an a/d ratio of 2.2, we observed a transition in the failure mode from shear failure to flexure failure with a v_f of 0.5% and 0.75% added to the beams. In this case, pure flexure failure took place with compression concrete crushing, as shown in Figure 11.

4 Discussion

From the results of the experimental tests that were conducted on high-strength reinforced concrete beams with discrete steel fibers in the concrete mixture, the effect of the various span–depth ratios on the relation between failure loads and the volume fraction of fibers (v_f) was investigated.

As shown in Table 11; Figure 12, for the lower percentages of v_f, less than 0.5%, the failure loads decreased by almost the same ratio (from 18% to 21%) at different a/d ratios. Moreover, by using a v_f of 0.75%, the load decreased by 26% at an a/d ratio of 2.2.

TABLE 11 Summary of failure loads under various a/d ratios.

Failure load	Beam
145	A-0
135	B-0
115	C-0
165	A-1
155	B-1
130	C-1
180	A-2
170	B-2
148	C-2
215	A-3
195	B-3
160	C-3

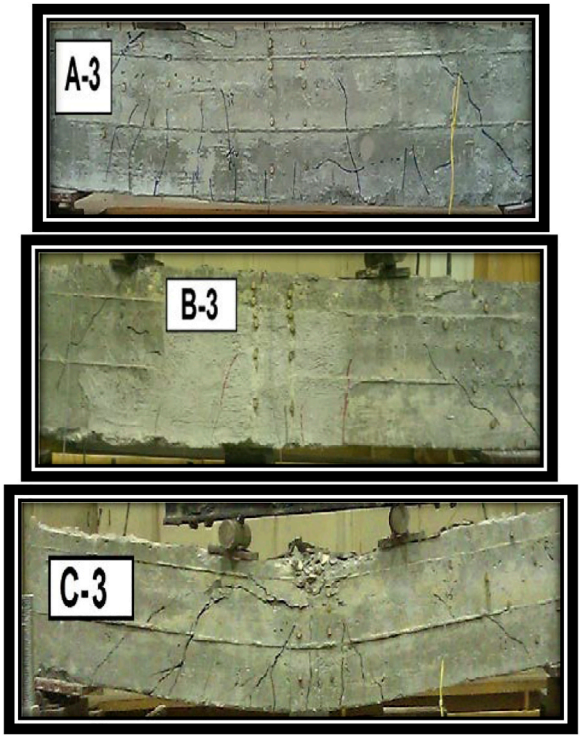

FIGURE 11
Propagation of cracks and modes of failure for HSFRC beams with a v_f of 0.75% and varying a/d ratios.

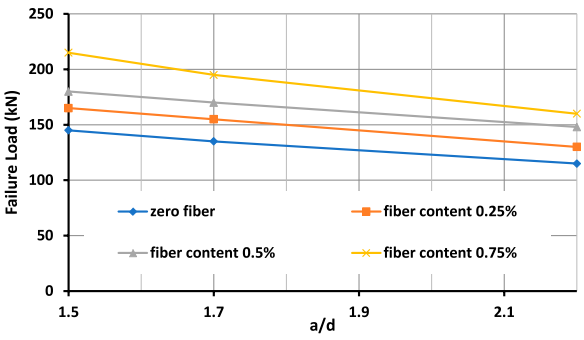

FIGURE 12
Influence of shear span-to-depth ratios on the tested beams.

At lower a/d ratios of 1.5 and 1.7, the behaviors of the HSRC beams were closer to a deep beam, on which the applied load was resisted by two major inclined diagonal struts formed from the compressive concrete part at this zone, called the disturbed region (D-region). That means that the concrete resistance by arch action at this zone does not show beam action, as shown in Figure 13. This behavior was the same for the HSFRC beams at lower a/d ratios of 1.5 and 1.7. The steel fibers acted as ties, which caused an increase in the shear strength and the flexure cracks which appeared, as shown in Figure 14. This clearly shows the effect of increasing the

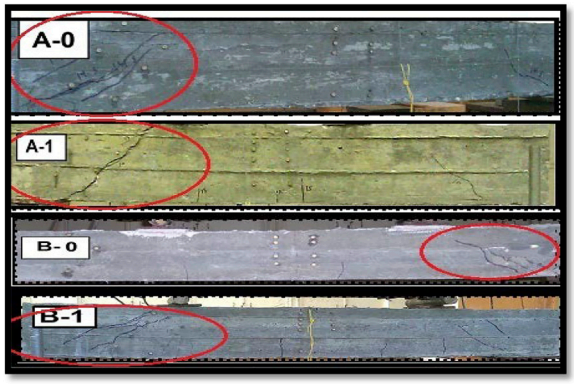

FIGURE 13
Influence of a/d ratio of 1.5 on the tested beams.

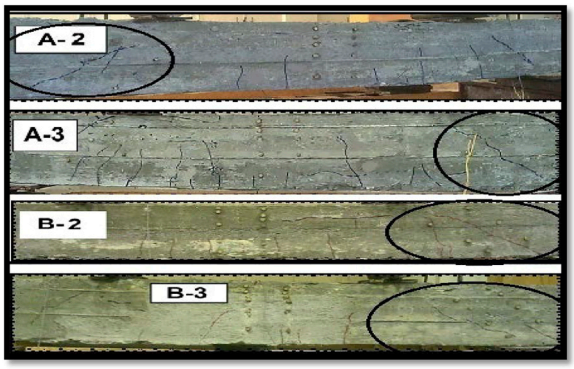

FIGURE 14
Influence of a/d ratio of 1.7 on the tested beams.

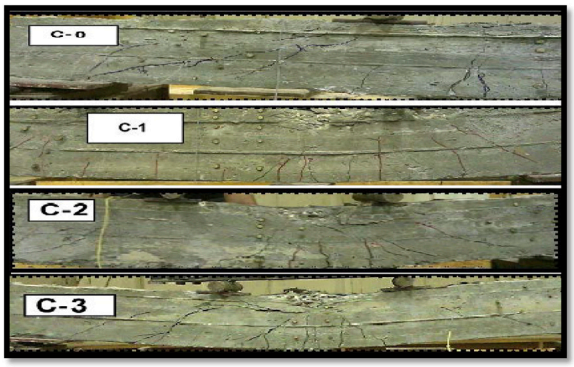

FIGURE 15
Influence of a/d ratio of 2.2 on the tested beams.

a/d ratio on all the beams. At that a/d ratio, the beams have both the disturbed and the beam regions under different loads, as shown in Figure 15. Additionally, the increase in fiber volume fraction

enhances the post-cracking stiffness of the tested beams at this a/d ratio, and the energy absorption ratio increased due to the bonding behavior between the fiber and the matrix.

Compared with previous studies that dealt with the same subject but using hook-end fibers, it was concluded that the deflection capability was increased with the use of corrugated steel fibers. This was due to the higher bond strength between the corrugated fibers, the concrete, and the bridging action of the fibers.

5 Conclusion

In the present study, discrete corrugated steel fibers comprising various fraction volumes were used to enhance the performance of high-strength, fiber-reinforced concrete beams. These beams were tested under various shear span-to-depth ratios to investigate their responses. Based on the experimental study, the following conclusions were derived:

- Under various shear span-to-depth ratios, the addition of steel fibers improves the mechanical properties of high-strength, fiber-reinforced concrete.
- The failure modes of reinforced HSC beams were similar to those of HSRF beams with low fiber content (0.25%).
- According to the results of this study, beams with a/d ratios smaller than 2.2 (Group A and Group B) fail in pure shear.
- Changing the a/d ratio to 2.2 causes beams to fail due to both flexure and shear–flexure modes, with multi-cracking observed, and major cracks propagated in the middle of the beam.
- The results showed that the high-strength concrete (HSRC) beams without fibers failed in shear at various a/d ratios smaller than 2.2, whereas HSFRC beams with an a/d ratio of 2.2 failed in pure flexure, with multi-cracking observed; therefore, these had higher crack width values and peak stress at fiber contents of 0.5% and 0.75%.
- The combination of stirrups and discrete steel fibers demonstrated a positive hybrid effect on the behavior of HSFRC beams.

Data availability statement

The raw data supporting the conclusion of this article will be made available by the authors, without undue reservation.

Author contributions

Conceptualization, AY; methodology, AY; validation, AY and MA; formal analysis, AY, SY, and AD; investigation, SY and AD; data curation, AY; writing—original draft preparation, SY and AD; writing—review and editing, AY and MA.

Conflict of interest

The authors declare that the research was conducted in the absence of any commercial or financial relationships that could be construed as a potential conflict of interest.

Publisher's note

References

Ahmed, S. F. U., Maalej, M., and Paramasivam, P. (2007). Flexural responses of hybrid steel–polyethylene fiber reinforced cement composites containing high volume fly ash. *Construction and Building Materials*. 21, 1088–1097. doi:10.1016/j.conbuildmat.2006.01.002

Astm A370 (2012). *Standard test methods and definitions for mechanical testing of steel products*. West Conshohocken, United State: ASTM.

Astm C 33-86 (1986). *Standard specification for concrete aggregates*. West Conshohocken, United State: Annual Book of ASTM Standards. ASTM.

Astm C-127 (2001). *Test method for density, relative density (specific gravity) and absorption of coarse aggregate*. West Conshohocken, PA, USA: ASTM.

Astm C-128 (2001). *Test method for density, relative density (specific gravity) and absorption of fine aggregate*. West Conshohocken, United State: ASTM.

Astm C188-14 (2009). *Standard test method for density of hydraulic cement*. West Conshohocken, United State: ASTM International, 109–188.

Astm C469/C469M-10 (2010). *Standard test method for static modulus of elasticity and Poisson's ratio of concrete in compression*. West Conshohocken, United State: ASTM International.

Astm C786/C786M-17 (2017). *Standard test method for fineness of hydraulic cement by the 150-_m (No. 100) and75-_m (No. 200) sieves*. West Conshohocken, United State: ASTM.

Bae, B.-I., Lee, M.-S., Choi, C.-S., Jung, H.-S., and Choi, H.-K. (2021). Evaluation of the ultimate strength of the ultra-high-performance fiber-reinforced concrete beams. *Applied Sciences*, 11, 2951. doi:10.3390/app11072951

Biolzi, L., Guerrini, G. L., and Rosati, G. (1997). Overall structural behavior of high strength concrete specimens. *Construction and Building Materials*. 11, 57–63. doi:10.1016/s0950-0618(96)00026-8

Brandt, A. M. (1985). On the optimal direction of short metal fibres in brittle matrix composites. *Journal of Materials Science*. 20, 3831–3841. doi:10.1007/BF00552371

Cao, M., and Khan, M. (2021). Effectiveness of multiscale hybrid fiber reinforced cementitious composites under single degree of freedom hydraulic shaking table. *Structural Concrete*. 22, 535–549. doi:10.1002/suco.201900228

Choi, W. C., Jung, K. Y., Jang, S. J., and Yun, H. D. (2019). The influence of steel fiber tensile strengths and aspect ratios on the fracture properties of high-strength concrete. *Materials* 12, 2105. doi:10.3390/ma12132105

Dinh, H. H. (2009). *Shear behavior of steel fiber reinforced concrete beams without stirrup reinforcement* (Ann Arbor, United State: College of Engineering—Civil and Environmental Engineering Department, University of Michigan). Ph.D. Thesis.

Geng, Y., and Leung, C. K. (1996). A microstructural study of fibre/mortar interfaces during fibre debonding and pull-out. *Journal of Materials Science*. 31, 1285–1294. doi:10.1007/BF00353108

Jang, S. J., Kang, D. H., Ahn, K. L., Park, W. S., Kim, S. W., and Yun, H. D. (2015). Feasibility of using high-performance steel fibre reinforced concrete for simplifying reinforcement details of critical members. *International Journal of Polymer Science*. 2015, 1–12. doi:10.1155/2015/850562

Khan, M., and Ali, M. (2020). Optimization of concrete stiffeners for confined brick masonry structures. *Journal of Building Engineering*. 32, 101689. doi:10.1016/j.jobe.2020.101689

Khan, M., Cao, M., Chu, S. H., and Ali, M. (2022). Properties of hybrid steel-basalt fiber reinforced concrete exposed to different surrounding conditions. *Construction and Building Materials*. 322, 126340. doi:10.1016/j.conbuildmat.2022.126340

Khan, M., Cao, M., Xie, C., and Ali, M. (2021). Hybrid fiber concrete with different basalt fiber length and content. *Structural Concrete*. 23, 346–364. doi:10.1002/suco.202000472

Kim, J. K., and Park, Y. D. (1994). Shear strength of reinforced high strength concrete beams without web reinforcement. *Magazine of Concrete Research*. 46, 7–16. doi:10.1680/macr.1994.46.166.7

Kou, S. C., and Poon, C. S. (2015). Effect of the quality of parent concrete on the properties of high performance recycled aggregate concrete. *Construction and Building Materials*. 77, 501–508. doi:10.1016/j.conbuildmat.2014.12.035

Kuder, K. G., and Shah, S. P. (2010). Processing of high-performance fiber-reinforced cement-based composites. *Construction and Building Materials*. 24, 181–186. doi:10.1016/j.conbuildmat.2007.06.018

Lantsoght, E. O. L. (2019). Database of shear experiments on steel fiber reinforced concrete beams without stirrups. *Materials* 12, 917. doi:10.3390/ma12060917

Lim, J. C., and Ozbakkaloglu, T. (2014). Influence of silica fume on stress–strain behavior of FRP-confined HSC. *Construction and Building Materials*. 63, 11–24. doi:10.1016/j.conbuildmat.2014.03.044

Lin, A. L. (2013). "Prediction of shear strength of fiber reinforced concrete beam of intermediate shear span,". In Chinese (Taipei, Taiwan: National Taiwan University). Master's Thesis (College of Engineering—Department of Civil Engineering.

Mansur, M. A., Ong, K. C. G., and Paramasivam, P. (1986). Shear strength of fibrous concrete beams without stirrups. *Journal of Structural Engineering*. 112, 2066–2079. doi:10.1061/(asce)0733-9445(1986)112:9(2066)

Ozbakkaloglu, T. (2013). Behavior of square and rectangular ultra high-strength concrete-filled FRP tubes under axial compression. *Composites Part B: Engineering*. 54, 97–111. doi:10.1016/j.compositesb.2013.05.007

Perceka, W., Liao, W. C., and Wu, Y. F. (2019). Shear strength prediction equations and experimental study of high strength steel fiber-reinforced concrete beams with different shear span-to-depth ratios. *Applied Science*. 9, 4790. doi:10.3390/app9224790

Savastano, H. J., Turner, A., Mercer, C., and Soboyejo, W. O. (2006). Mechanical behavior of cement-based materials reinforced with sisal fibers. *Journal of Materials Science*, 41, 6938–6948. doi:10.1007/s10853-006-0218-1

Shahnewaz, M., and Alam, M. S. (2020). Genetic algorithm for predicting shear strength of steel fiber reinforced concrete beam with parameter identification and sensitivity analysis. *Journal of Building Engineering*. 29, 101205. doi:10.1016/j.jobe.2020.101205

Song, P. S., and Hwang, S. (2004). Mechanical properties of high strength steel fiber-reinforced concrete. *Construction and Building Materials*. 18, 669–673. doi:10.1016/j.conbuildmat.2004.04.027

Sudin, R., and Swamy, N. (2006). Bamboo and wood fibre cement composites for sustainable infrastructure regeneration. *Journal of Materials Science*. 41, 6917–6924. doi:10.1007/s10853-006-0224-3

Swamy, R. N., and Bahia, H. M. (1985). The effectiveness of steel fibers as shear reinforcement. *International Concrete Abstracts Portal*. 7, 35–40. doi:10.14359/51686736

Toutanji, H., Delatte, N., Aggoun, S., Duval, R., and Danson, A. (2004). Effect of supplementary cementitious materials on the compressive strength and durability of short-term cured concrete. *Cement and Concrete Research*. 34, 311–319. doi:10.1016/j.cemconres.2003.08.017

Vincent, T., and Ozbakkaloglu, T. (2015). Influence of shrinkage on compressive behavior of concrete-filled FRP tubes: An experimental study on interface gap effect. *Construction and Building Materials*. 75, 144–156. doi:10.1016/j.conbuildmat.2014.10.038

Yoo, D. Y., Yuan, T., Yang, J. M., and Yoon, Y. S. (2017). Feasibility of replacing minimum shear reinforcement with steel fibers for sustainable high-strength concrete beams. *Engineering Structures*. 147, 207–222. doi:10.1016/j.engstruct.2017.06.004

Yun, H.-D., Jeong, G.-Y., and Choi, W.-C. (2022). Shear strengthening of high strength concrete beams that contain hooked-end steel fiber. *Materials* 15, 17. doi:10.3390/ma15010017

Yurtseven, A. E. (2004). "Determination of mechanical properties of hybrid fiber einforced concrete," *Master's thesis* (Ankara, Turkey: Middle East Technical University).

Zhao, J., Liang, J., Chu, L., and Shen, F. (2018). Experimental study on shear behavior of steel fiber reinforced concrete beams with high-strength reinforcement. *Materials* 11, 1682. doi:10.3390/ma11091682